

**Supplemental Figure S1. Spike removal from field recordings**

(A) (*Top*) Field recordings from superficial OT layers. Superficial layer spikes occur in 2-4 ms bursts. (*Middle*) Field recordings following the spike removal procedure (see Materials and Methods, main text). (*Bottom*) The local field potential (LFP) after spike removal, low-pass filtering with a high cutoff at 200 Hz, and downsampling to 1kHz (see Materials and Methods, main text).

(B) Same as in (A), but for recordings from the deep OT layers. Deep layer spikes manifest as large amplitude single (non-bursting) spikes. Other conventions are as in panel (A).

**Supplemental Figure S2. Visually induced R-spectra (averaged across sites)**

Visually induced average R-spectra for the population of superficial (blue, n=25) and deep (red, n=32) layer sites used in all of the results presented. Dotted lines: 95% confidence intervals. R-spectra were normalized to their maximum value (at that site) before being averaged across sites to permit comparing frequencies of induced peak gamma power of superficial and deep layer spectra on the same axis. Other conventions are as in Figure 3 (main text).

**Supplemental Figure S3. Fisher information for induced gamma LFP power and spike rates.**

(A) Fisher information for gamma LFP power (dashed line) and spike rates (solid line) as a function of distance from the receptive field center (degrees) computed based on the population of spike and LFP tuning curves in the superficial layers (n=28). Dotted

lines: 95% confidence intervals across sites. Fisher information was computed after centering the tuning curve for each site at its maximum value, and normalized (divided) by the number of sites in the population.

(B) Same as in (A) but for tuning curves in the deep layer (n=42).

**Supplemental Figure S4.** Average spike-field coherence evoked by auditory stimuli, shuffled responses, and at a subset of sites showing low-gamma coherence in the superficial and deep layers.

(A) Population average of the spike-field coherence evoked by auditory stimuli in superficial (blue), and deep (red) layers. Region between dotted lines: 95% confidence intervals across sites. Other conventions are as in Fig. 9 (main text).

(B) Spike-field coherence was not an artifact of stimulus-locked oscillations. Spike-field coherence in superficial (thick blue line) and deep (thick red line) layer sites to randomly matched trials of visually evoked spikes and LFPs. Spike-field coherence was abolished as a result of shuffling LFP and spike trials. Region between dotted lines: 95% confidence intervals across sites.

(C) Population average of the spike-field coherence evoked by visual stimuli in the subset of sites at which coherence magnitude was greatest in the low-gamma band (n=23/25, superficial, and n=18/32, deep). Other conventions are the same as in (A).

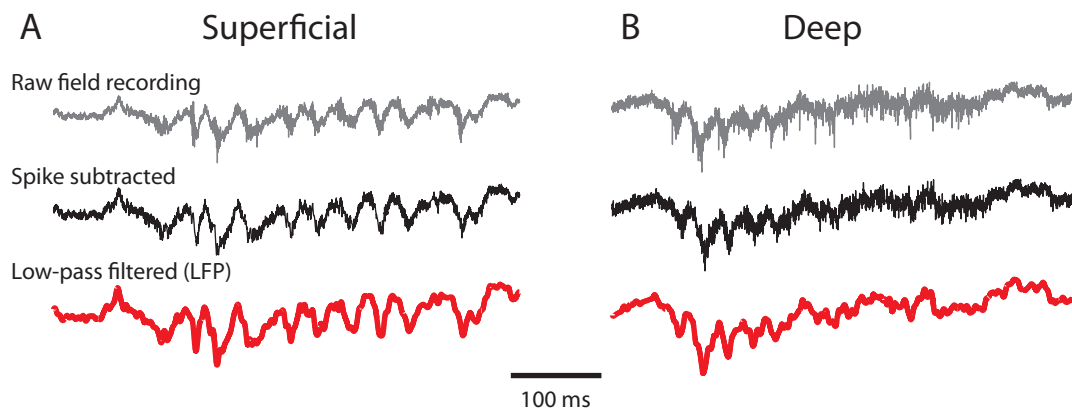
(D) Same as in (C), but for sites at which coherence evoked by auditory stimuli was greatest in the low-gamma band (n=10/11, superficial, and n=10/17, deep).

**Supplemental Figure S5.** Spike-field coherence in the superficial layers computed by including all spikes in each burst.

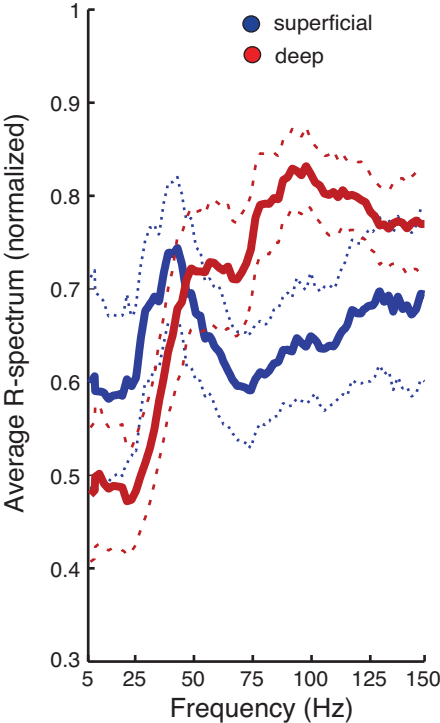
(A) Population average of the spike-field coherence evoked by visual stimuli in superficial layers computed by including all spikes in each burst (dashed line), or with only the first spike in each burst (solid line). While absolute SFC magnitudes were different between the two methods, the relative distribution of SFC across frequencies was identical (see Materials and Methods).

(B) Same as in (A), but for coherence evoked by auditory stimuli.

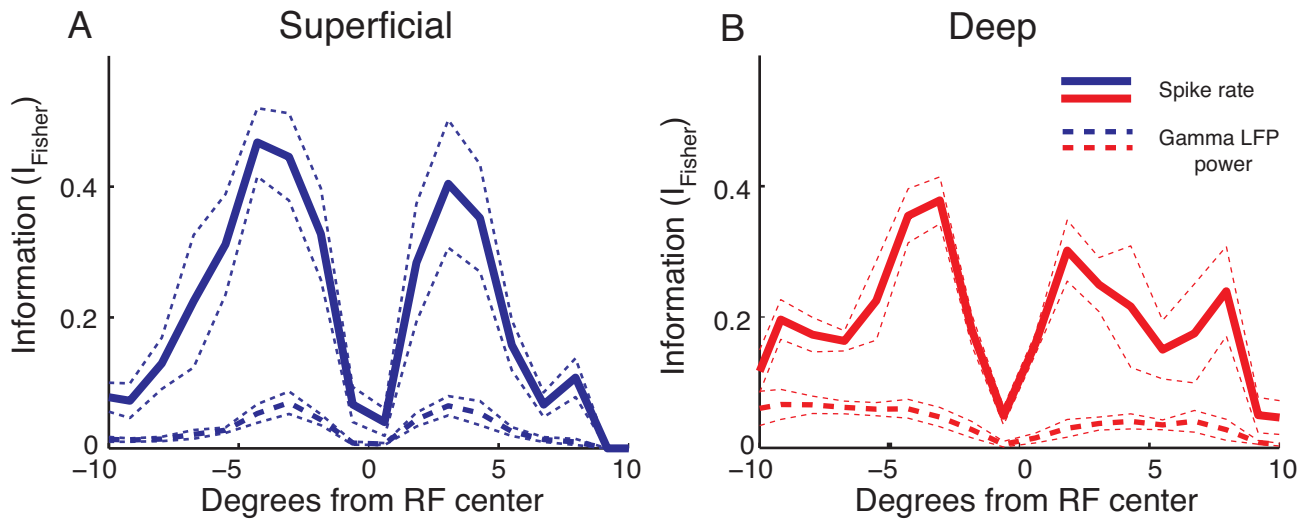
# Supplemental Figure S1



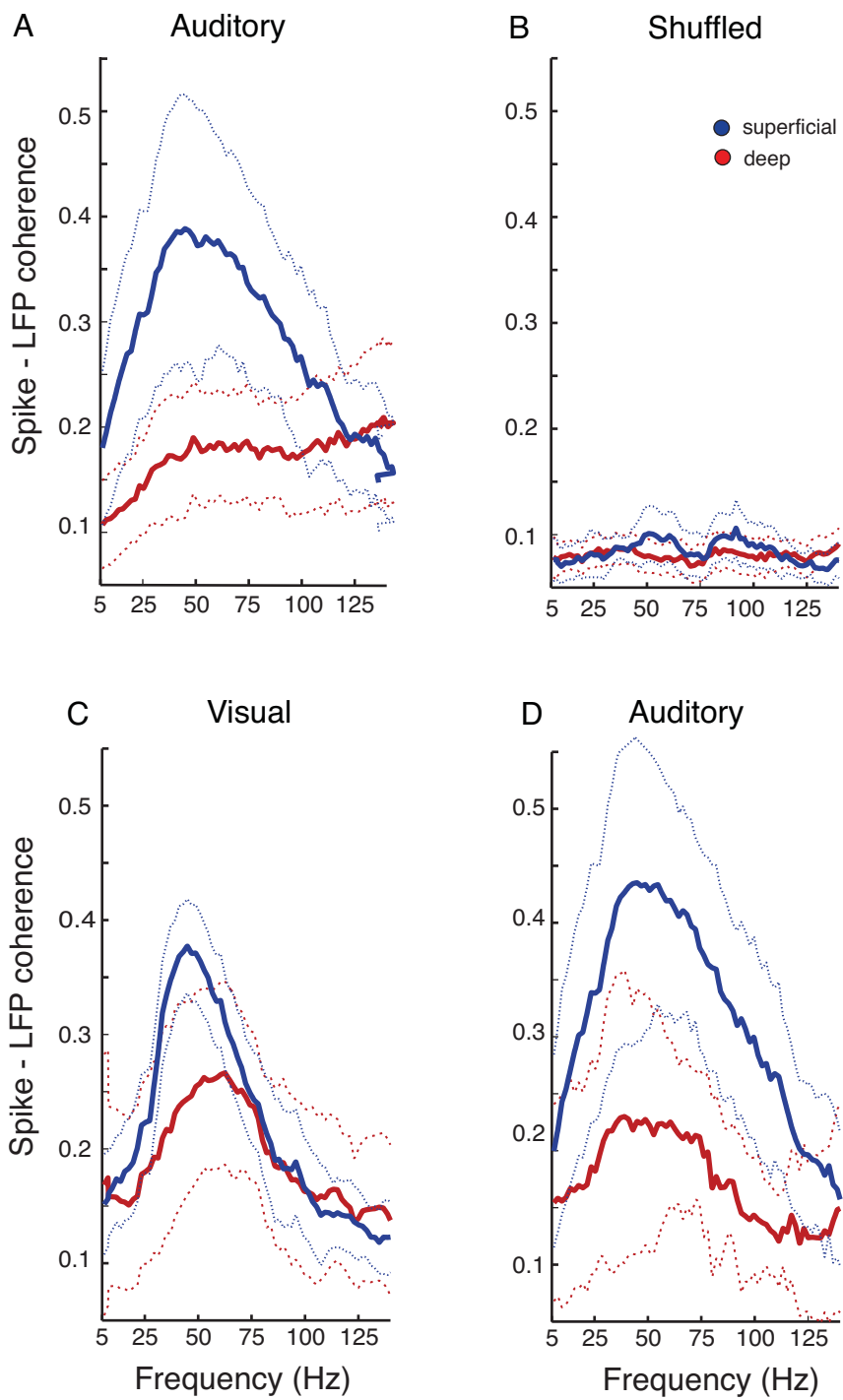
# Supplemental Figure S2



# Supplemental Figure S3



# Supplemental Figure S4



# Supplemental Figure S5

